Journal of Organometallic Chemistry, 341 (1988) 473–483
Elsevier Sequoia S.A., Lausanne – Printed in The Netherlands

Ligand substitution in $[Co_xRh_{4-x}(CO)_{12}]$ ($x = 3$ or 2) with tertiary phosphines or phosphites, including the X-ray structure of $[Co_2Rh_2(CO)_{11}(PPh_3)]$ *

Maria Bojczuk, Brian T. Heaton*, S. Johnson,

Department of I.P.I. Chemistry, P.O. Box 147, The University, Liverpool, L69 3BX (Great Britain)

Carlo A. Ghilardi and Annabella Orlandini

C.N.R. Istituto per lo Studio della Stereochimica ed Energetica dei Composti di Coordinazione, Via J. Nardi 39, 50132 Firenze (Italy)

(Received September 1st, 1987)

Abstract

Ligand substitution of the mixed-metal clusters $[Co_3Rh(CO)_{12}]$ and $[Co_2Rh_2(CO)_{12}]$ with triphenylphosphine or triphenylphosphite has been studied by NMR spectrometry and shown to occur preferentially at the rhodium centres. The molecular structure of $[Co_2Rh_2(CO)_{11}(PPh_3)]$ has been determined by X-ray crystallography, and shown to be related to that of the parent cluster: both rhodium atoms are in the basal plane and the triphenylphosphine is attached to rhodium in an axial site.

Introduction

There is now a variety of homo- and hetero-metallic tetranuclear clusters which are derived from the C_{3v} structure of $[M_4(\mu\text{-}CO)_3(CO)_9]$ (M = Co [1,2] or Rh [2]), Table 1. For this particular structure, the following features are of interest: (a) the stereochemistry of the products resulting on CO replacement by various other ligands, (b) the occupancy of apical and basal sites (Fig. 1) by the different metals in heterometallic clusters, and (c) preferential metal selectivity for CO substitution in heterometallic clusters.

Despite recent calculations [20], which show that for $[M_4(CO)_{12}]$ (M = Co or Rh), the least sterically hindered sites are the radial carbonyl sites (Fig. 1), the large

* Dedicated to Professor Colin Eaborn, in recognition of his important contributions to organometallic chemistry.

0022-328X/88/$03.50

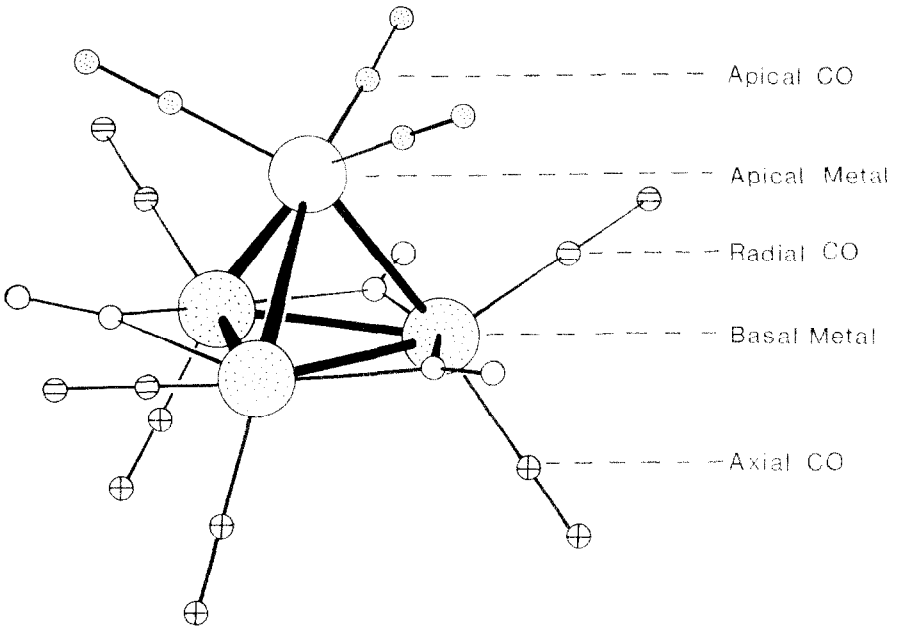

Fig. 1. Classification of ligands/metals for clusters having structures related to the C_{3v} structure of $[M_4(CO)_{12}]$ (M = Co [1,2] or Rh [2]).

majority of mono-substituted clusters in Table 1 have ligands in an axial site, *trans* to the formal M_{basal}–M_{apical} bond. As discussed earlier [21], this seems to be due to an electronic effect. In homometallic clusters, the sites occupied by the second and third incoming ligands depend upon the size of the ligand, with small ligands (e.g. H or $P(OMe)_3$) entering axial sites and larger ligands progressively substituting on different basal metal atoms but going as far away from the first ligand as possible [22]; the fourth ligand is obliged to occupy an apical site which results in the two ligands on the basal metals on that $M_{apical}(M_{basal})_2$-triangular face going into axial sites with the other ligand in the basal plane occupying a radial site to minimize steric effects. For the heterometallic analogues, there is a marked tendency, even for bulky ligands, to substitute in axial sites on the basal metal atom. Although the H-site occupancy has only been unambiguously established for $[HFeCo_3(CO)_9(P(OMe)_3)_3]$ [18], it seems probable that all the other hydride/ligand substituted analogues also have μ_3-H below the basal M_3-plane; this causes the radial carbonyls to bend towards the apical metal atom and provides more room for incoming ligands to occupy the axial sites. All these data with ligand/metal site occupancies are summarized in Table 1.

It was established some time ago from X-ray crystallographic [23] and IR measurements [24], and subsequently confirmed by NMR spectrometry [25], that in the mixed clusters, $[M'_xM_{4-x}(CO)_{12}]$ (M′ = M = Co, Rh, or Ir; $x = 1$, 2 or 3), the tendency towards basal site occupancy is rhodium > cobalt > iridium. For $[HM'M_3(CO)_{12}]$ (M′ = Fe, Ru or Os; M = Co or Rh), the apical site seems always to be occupied by M′; Ru is also found in the apical site in $[H_3Ru_2Rh_2(CO)_{12}]$ [26]. The reasons for this are not obvious, but are probably related to the greater

Table 1

X-ray crystallographically characterised clusters containing monodentate ligands derived from the C_{3v} structure of $[M_4(\mu\text{-}CO)_3(CO)_9]$ (M = Co [1,2] or Rh [2])

Cluster	Apical M	Basal M	Site of ligand	Reference
$[Co_4(CO)_{11}(C(O)Me)]$	Co	Co	axial	3
$[Co_4(CO)_{11}I]^-$	Co	Co	98% apical, 2% axial	4
$[Co_4(CO)_{11}(PPh_3)]$	Co	Co	axial	5
$[Co_4(CO)_{11}(PMe_3)]$	Co	Co	axial	6
$[Co_4(CO)_{10}(P(OMe)_3)_2]$	Co	Co	2 axial	5
$[Co_4(CO)_{10}\{P(CH_2CHCH_2)Me_2\}_2]$	Co	Co	1 axial, 1 apical (*trans*)	7
$[Rh_4(CO)_{10}(PPh_3)_2]$	Rh	Rh	1 axial, 1 radial	8
$[Rh_4(CO)_9P(OPh)_3)_3]$	Rh	Rh	1 axial, 2 radial	8
$[Rh_4(CO)_8(P(OPh)_3)_4]$	Rh	Rh	2 axial, 1 radial, 1 apical	9
$[Ir_4(CO)_{11}Br]^-$	Ir	Ir	axial	10
$[Ir_4(CO)_{11}(CO_2Me)]^-$	Ir	Ir	axial	11
$[Ir_4(CO)_{11}\{Ir_4(CO)_{11}\}]^{2-}$	Ir	Ir	axial	12
$[Ir_4(CO)_{10}H_2]^{2-}$	Ir	Ir	2 axial	13
$[Ir_4(CO)_{10}(PPh_3)_2]$	Ir	Ir	1 axial, 1 radial	14
$[Ir_4(CO)_9(PPh_3)_3]$	Ir	Ir	1 axial, 2 radial	14
$[Ir_4(CO)_8(PMe_3)_4]$	Ir	Ir	2 axial, 1 radial, 1 apical	15
$[Ir_4(CO)_8(PMe_2Ph)_4]$	Ir	Ir	2 axial, 1 radial, 1 apical	16
$[HFeCo_3(CO)_{10}(PPh_3)_2]$	Fe	Co	2 axial	17
$[HFeCo_3(CO)_9P(OMe)_3)_3]$	Fe	Co	3 axial	18
$[HFeCo_3(CO)_9(PMe_2Ph)_3]$	Fe	Co	2 axial, 1 apical (*trans*)	6
$[HRuCo_3(CO)_{10}(PPh_3)_2]$	Ru	Co	2 axial	19
$[HRuRh_3(CO)_{10}(PPh_3)_2]$	Ru	Rh	2 axial	19

tendency of cobalt and rhodium to be involved with bridging carbonyls and thus favour basal site occupancy.

For clusters of the type $[HM'M_3(CO)_{12}]$, ligand substitution preferentially occurs on the basal metal atom and appears to be independent of the metal combination. This should be contrasted with monomeric carbonyls, which show that the rate of CO replacement is faster for second than for first or third row metals [27], and ligand replacement also occurs preferentially at ruthenium in the mixed-metal clusters, $[Fe_xRu_{3-x}(CO)_{12}]$ ($x = 1$ or 2) [28].

It was thus of interest to establish whether substitution occurred preferentially at cobalt or rhodium in $[Co_xRh_{4-x}(CO)_{12}]$ ($x = 3$ or 2), and to see if the pattern of isomers established for the homo-metallic $[M_4(CO)_{12}]$ clusters on progressive substitution was retained in the mixed cobalt/rhodium clusters. We have used ^{31}P NMR spectroscopy to follow the course of the substitution reactions with triphenylphosphine and triphenylphosphite; in order to unambiguously distinguish between radial/axial substitution we have carried out an X-ray structural determination of $Co_2Rh_2(CO)_{11}(PPh_3)$. After the completion of this work [29], a related NMR study of the reaction of PEt_3 with $Co_2Rh_2(CO)_{12}$ appeared [30] and their conclusions are in accord with our results now reported.

Results and discussion

Ligand substitution in $[Co_3Rh(CO)_{12}]$

(a) With PPh_3. The reaction of equimolar amounts of $[Co_3Rh(CO)_{12}]$ with PPh_3 in hexane was immediate and low temperature crystallisation gave black

Table 2

NMR data for $[Co_xRh_{4-x}(CO)_{12-y}L_y]$ ($x = 3$ or 2; $y = 1$ or 2; L = PPh_3 or $P(OPh)_3$) and related derivatives [a]

	$\delta(P_{ax})$ [b] (ppm)	$\delta(P_{rad})$ [b] (ppm)	$^1J(Rh-P_{ax})$ (Hz)	$^1J(Rh-P_{rad})$ (Hz)	$^2J(Rh_{bas}-P_{rad})$ (Hz)	Reference
$[Rh_4(CO)_{11}(PPh_3)]$	+24.1		119			8
$[Rh_4(CO)_{11}(PPh_3)]$		+24.9		134		8
$[Co_3Rh(CO)_{11}(PPh_3)]$	+31.0		122.4			this work
$[Co_2Rh_2(CO)_{11}(PPh_3)]$	+27.1		124.0			this work
$[Rh_4(CO)_{10}(PPh_3)_2]$	+18.5	+32.4	127	138.2	12	8
$[Rh_4(CO)_{10}(PPh_3)_2]$	+28.2		125			8
$[Co_3Rh(CO)_{10}(PPh_3)_2]$	+30.3	+28.6	118.7	136.2		this work
$[Co_2Rh_2(CO)_{10}(PPh_3)_2]$	+26.9	+28.8	124.0	133.3	12.7	this work
$[Co_2Rh_2(CO)_{11}(PEt_3)]$	+31.5		116			30
$[Co_2Rh_2(CO)_{10}(PEt_3)_2]$	+33.5	+25.8	117	136		30
$[Rh_4(CO)_{11}\{P(OPh)_3\}]$	+100.9		205			8
$[Co_3Rh(CO)_{11}\{P(OPh)_3\}]$	+107.4		210.3			this work
$[Co_3Rh(CO)_{11}\{P(OPh)_3\}]$		+111.5		260.6		this work
$[Co_2Rh_2(CO)_{11}\{P(OPh)_3\}]$	+106.1		210.2			this work
$[Rh_4(CO)_{10}\{P(OPh)_3\}_2]$	+102.2	+116.6	212	260	18	8
$[Co_2Rh_2(CO)_{10}\{P(OPh)_3\}_2]$	+106.8	+117.3	218.8	259.1	16.9	this work

[a] L is always bonded to Rh. [b] Referenced to H_3PO_4 (85% in D_2O).

crystals which had an analysis consistent with the formulation, $[Co_3Rh(CO)_{11}(PPh_3)]$ (**1**). The ^{31}P NMR spectrum of **1** contains a strong doublet ($\delta(P)$ 30.3 ppm; $^1J(Rh-P)$ 122.4 Hz). This is consistent with PPh_3 occupying an axial site, since in $[Rh_4(CO)_{11}(PPh_3)]$ the value for $^1J(Rh-P_{ax})$ is 119.0 Hz, whereas the value for $^1J(Rh-P_{rad})$ is ca. 20 Hz higher [8]. Additionally, the ^{31}P NMR spectrum of **1** contains two equally intense but much weaker doublets ($\delta(P)$ 30.3 and 28.6 ppm; $^1J(Rh-P)$ 118.7 and 136.2 Hz, respectively). Since both the δ and $^1J(Rh-P)$ values are in accord with axial and radial substitution, respectively, these two resonances could arise from $[Co_3Rh(CO)_{10}(PPh_3)_2]$, with both triphenylphosphine molecules attached to the rhodium. Such a product could result from a disproportionation reaction, which has been shown to occur readily in tetranuclear clusters [8,31].

(b) With $P(OPh)_3$. Both the IR and ^{31}P NMR spectra (Table 2) are consistent with the reaction of an equimolar amount of $P(OPh)_3$ with $[Co_3Rh(CO)_{12}]$ resulting in substitution on rhodium to give the axial isomer of $[Co_3Rh(CO)_{11}(P(OPh)_3)]$ (**2**). Unfortunately, crystals could not be obtained, but the ^{31}P NMR spectrum at $-50\,^\circ C$ consists of a clean doublet ($\delta(P)$ 110.0 ppm; $^1J(Rh-P)$ 210.3 Hz) which is similar to the value of $^1J(Rh-P)$ 205 Hz obtained for $[Rh_4(CO)_{11}(P(OPh)_3)]$ [8]. Subsequent ^{31}P NMR spectra of **2** at room temperature showed the appearance of a second doublet ($\delta(P)$ 113.1 ppm; $^1J(Rh-P)$ 260.6 Hz) which could be assigned to a $Rh-P_{rad}$ isomer. This equilibrium has previously been observed in solution for $[Ir_4(CO)_{11}L]$ (L = PPh_2Me or $PPhMe_2$) [32] and $[Rh_4(CO)_{11}(PPh_3)]$ [8].

Ligand substitution in $[Co_2Rh_2(CO)_{12}]$

(a) With PPh_3. The reaction of 1 mol of PPh_3 with 1 mol of $[Co_2Rh_2(CO)_{12}]$ in hexane produced an immediate black precipitate which has been shown by X-ray

crystallography, vide infra, to be $[Co_2Rh_2(CO)_{11}(PPh_3)]$ (**3**), with PPh_3 bonded to rhodium in an axial site, and with both rhodium atoms in the basal plane as found in $[Co_2Rh_2(CO)_{12}]$.

The ^{31}P NMR spectrum of **3** consists of a sharp doublet at 27.1 ppm, ^1J(Rh–P) 124.0 Hz. This value of the coupling constant is entirely consistent with the phosphine being in an axial site (Table 1), which has now been confirmed from X-ray crystallographic studies, vide infra.

Further reaction with PPh_3 (1 mol) gave $[Co_2Rh_2(CO)_{10}(PPh_3)_2]$ (**4**), which from ^{31}P NMR measurements has both phosphine ligands on different rhodium atoms: one in an axial site ($\delta(P_{ax})$ 26.9 ppm; $^1J(Rh-P_{ax})$ 124.0 Hz) and one in a radial site ($\delta(P_{rad})$ 28.8 ppm; ^1J(Rh–P) 133.4 Hz; $^2J(Rh_{bas} - P_{rad})$ 12.7 Hz).

(b) With P(OPh)$_3$. As found for the reaction of $P(OPh)_3$ with $[Co_3Rh(CO)_{12}]$, no crystalline products could be isolated from the progressive addition of 1 and 2 mol of $P(OPh)_3$ to $[Co_2Rh_2(CO)_{12}]$. After the addition of 1 mol of $P(OPh)_3$ to 1 mol of $[Co_2Rh_2(CO)_{12}]$, the ^{31}P NMR spectrum showed the presence of two doublets, which are attributed to the rhodium-substituted axial (δ(P) 106.1 ppm; ^1J(Rh–P) 210.2 hz) and radial (δ(P) 111.5 ppm; ^1J(Rh–P) 260.6 Hz) isomers of $[Co_2Rh_2(CO)_{11}(P(OPh)_3)]$ (**5**). Further addition of 1 mol of $P(OPh)_3$ gives $[Co_2Rh_2(CO)_{10}(P(OPh)_3)_2]$ (**6**), for which there is only evidence for one isomer with a rhodium-substituted axial (δ(P) 109.5 ppm; ^1J(Rh–P) 218.8 Hz) and radial (δ(P) 120.0 ppm; ^1J(Rh–P) 259.1 Hz; $^2J(Rh_{bas}$–P) 16.9 Hz) triphenylphosphite ligand.

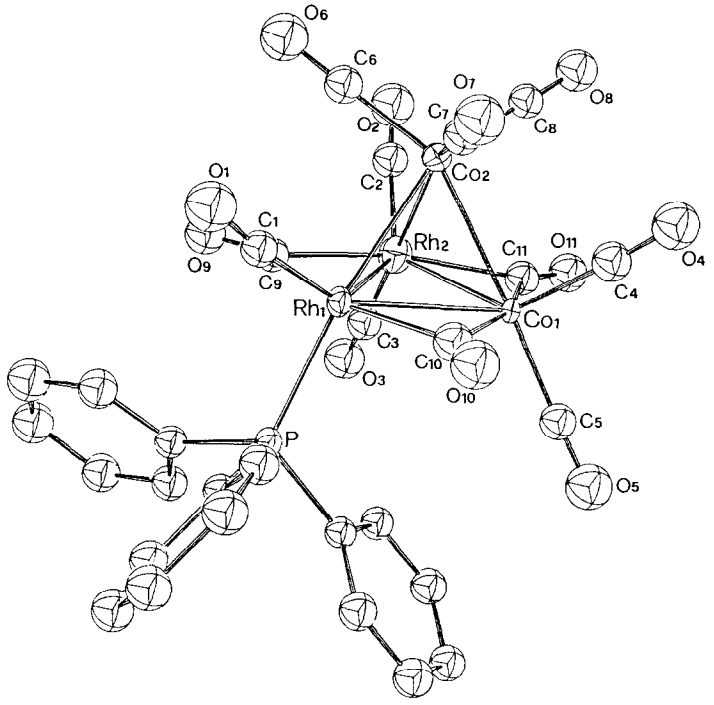

Fig. 2. ORTEP plot and numbering scheme of the cluster $[Co_2Rh_2(CO)_{11}(PPh_3)]$.

Table 3. Selected bond distances (Å) and angles (deg) for **3**

Rh(1)–Rh(2)	2.663(2)	Co(2)–C(6)	1.81(2)
Rh(1)–Co(1)	2.653(2)	Co(2)–C(7)	1.78(2)
Rh(1)–Co(2)	2.617(2)	Co(2)–C(8)	1.83(2)
Rh(1)–P	2.327(3)	C(1)–O(1)	1.13(2)
Rh(1)–C(1)	1.84(1)	C(2)–O(2)	1.11(2)
Rh(1)–C(9)	2.05(1)	C(3)–O(3)	1.16(2)
Rh(1)–C(10)	2.05(2)	C(4)–O(4)	1.14(2)
Rh(2)–Co(1)	2.633(2)	C(5)–O(5)	1.13(2)
Rh(2)–Co(2)	2.567(2)	C(6)–O(6)	1.11(2)
Rh(2)–C(2)	1.80(2)	C(7)–O(7)	1.15(2)
Rh(2)–C(3)	1.82(2)	C(8)–O(8)	1.11(2)
Rh(2)–C(9)	2.06(1)	C(9)–O(9)	1.16(2)
Rh(2)–C(11)	2.03(1)	C(10)–O(10)	1.14(2)
Co(1)–Co(2)	2.557(2)	C(11)–O(11)	1.14(2)
Co(1)–C(4)	1.80(2)	P–C(1,1)	1.82(1)
Co(1)–C(5)	1.83(2)	P–C(1,2)	1.83(1)
Co(1)–C(10)	1.98(2)	P–C(1,3)	1.82(1)
Co(1)–C(11)	1.97(2)		
Rh(2)–Rh(1)–Co(1)	59.4(1)	Rh(2)–Co(1)–C(10)	110.5(5)
Rh(2)–Rh(1)–Co(2)	58.2(1)	Rh(2)–Co(1)–C(11)	49.7(4)
Rh(2)–Rh(1)–P	114.7(1)	Co(2)–Co(1)–C(4)	87.0(5)
Rh(2)–Rh(1)–C(1)	133.9(5)	Co(2)–Co(1)–C(5)	177.4(5)
Rh(2)–Rh(1)–C(9)	49.9(4)	Co(2)–Co(1)–C(10)	84.3(5)
Rh(2)–Rh(1)–C(10)	107.2(4)	Co(2)–Co(1)–C(11)	85.9(4)
Co(1)–Rh(1)–Co(2)	58.0(1)	C(4)–Co(1)–C(5)	95.3(7)
Co(1)–Rh(1)–P	113.4(1)	C(4)–Co(1)–C(10)	95.5(7)
Co(1)–Rh(1)–C(1)	140.0(4)	C(4)–Co(1)–C(11)	101.2(7)
Co(1)–Rh(1)–C(9)	109.2(4)	C(5)–Co(1)–C(10)	94.3(7)
Co(1)–Rh(1)–C(10)	47.8(4)	C(5)–Co(1)–C(11)	94.8(7)
Co(2)–Rh(1)–P	170.4(1)	C(10)–Co(1)–C(11)	160.1(6)
Co(2)–Rh(1)–C(1)	94.8(4)	Rh(1)–Co(2)–Rh(2)	61.8(1)
Co(2)–Rh(1)–C(9)	83.6(4)	Rh(1)–Co(2)–Co(1)	61.7(1)
Co(2)–Rh(1)–C(10)	81.4(4)	Rh(1)–Co(2)–C(6)	93.4(5)
P–Rh(1)–C(1)	94.7(4)	Rh(1)–Co(2)–C(7)	95.4(5)
P–Rh(1)–C(9)	96.3(4)	Rh(1)–Co(2)–C(8)	152.3(5)
P–Rh(1)–C(10)	95.7(4)	Rh(2)–Co(2)–Co(1)	61.8(1)
C(1)–Rh(1)–C(9)	94.4(6)	Rh(2)–Co(2)–C(6)	152.7(5)
C(1)–Rh(1)–C(10)	104.1(6)	Rh(2)–Co(2)–C(7)	95.1(5)
C(9)–Rh(1)–C(10)	157.0(6)	Rh(2)–Co(2)–C(8)	96.0(5)
Rh(1)–Rh(2)–Co(1)	60.1(1)	Co(1)–Co(2)–C(6)	97.4(5)
Rh(1)–Rh(2)–Co(2)	60.0(1)	Co(1)–Co(2)–C(7)	152.6(5)
Rh(1)–Rh(2)–C(2)	134.0(5)	Co(1)–Co(2)–C(8)	94.0(5)
Rh(1)–Rh(2)–C(3)	115.5(5)	C(6)–Co(2)–C(7)	98.8(7)
Rh(1)–Rh(2)–C(9)	49.3(4)	C(6)–Co(2)–C(8)	103.5(7)
Rh(1)–Rh(2)–C(11)	107.9(4)	C(7)–Co(2)–C(8)	103.4(7)
Co(1)–Rh(2)–Co(2)	58.9(1)	Rh(1)–P–C(1,1)	112.6(4)
Co(1)–Rh(2)–C(2)	131.6(5)	Rh(1)–P–C(1,2)	114.4(3)
Co(1)–Rh(2)–C(3)	119.9(5)	Rh(1)–P–C(1,3)	116.9(3)
Co(1)–Rh(2)–C(9)	109.4(4)	C(1,1)–P–C(1,2)	106.8(4)
Co(1)–Rh(2)–C(11)	47.9(4)	C(1,1)–P–C(1,3)	102.0(4)
Co(2)–Rh(2)–C(2)	87.7(5)	C(1,2)–P–C(1,3)	102.8(4)
Co(2)–Rh(2)–C(3)	175.5(5)	Rh(1)–C(1)–O(1)	174.7(14)
Co(2)–Rh(2)–C(9)	84.5(4)	Rh(2)–C(2)–O(2)	175.9(16)
Co(2)–Rh(2)–C(11)	84.5(4)	Rh(2)–C(3)–O(3)	175.7(15)
C(2)–Rh(2)–C(3)	95.8(7)	Co(1)–C(4)–O(4)	176.4(15)

Table 3 (continued)

C(2)–Rh(2)–C(9)	99.9(6)	Co(1)–C(5)–O(5)	177.0(15)
C(2)–Rh(2)–C(11)	99.8(7)	Co(2)–C(6)–O(6)	179.0(15)
C(3)–Rh(2)–C(9)	92.1(6)	Co(2)–C(7)–O(7)	178.6(15)
C(3)–Rh(2)–C(11)	97.6(6)	Co(2)–C(8)–O(8)	176.1(14)
C(9)–Rh(2)–C(11)	157.1(6)	Rh(1)–C(9)–O(9)	143.6(12)
Rh(1)–Co(1)–Rh(2)	60.5(1)	Rh(2)–C(9)–O(9)	135.5(12)
Rh(1)–Co(1)–Co(2)	60.3(1)	Rh(1)–C(9)–Rh(2)	80.9(5)
Rh(1)–Co(1)–C(4)	131.5(5)	Rh(1)–C(10)–O(10)	138.9(14)
Rh(1)–Co(1)–C(5)	117.2(5)	Co(1)–C(10)–O(10)	138.7(14)
Rh(1)–Co(1)–C(10)	50.1(5)	Rh(1)–C(10)–Co(1)	82.1(6)
Rh(1)–Co(1)–C(11)	110.1(4)	Rh(2)–C(11)–O(11)	135.6(13)
Rh(2)–Co(1)–Co(2)	59.3(1)	Co(1)–C(11)–O(11)	141.9(13)
Rh(2)–Co(1)–C(4)	133.3(5)	Rh(2)–C(11)–Co(1)	82.4(6)
Rh(2)–Co(1)–C(5)	119.5(5)		

All the NMR spectroscopic data for these and related homo- and hetero-rhodium cluster derivatives are summarized in Table 2.

The reaction of both $[Co_3Rh(CO)_{12}]$ and $[Co_2Rh_2(CO)_{12}]$ with an excess of ($L = PPh_3$ or $P(OPh)_3$) was not further investigated in detail, but it seems probable that, by analogy with Horvath's results [30], fragmentation occurs.

Description of the structure of $[Co_2Rh_2(CO)_{11}(PPh_3)]$ (3)

The molecular structure consists of discrete cluster units of $[Co_2Rh_2(CO)_{11}(PPh_3)]$. Figure 2 shows a perspective view of the cluster molecule, with selected bond distances and angles reported in Table 3. The structure consists of a tetrahedral Co_2Rh_2 core, in which a $Co(CO)_3$ apical group is symmetrically linked by metal–metal bonds to a basal Rh_2Co triangular fragment. The three metal atoms at the vertices of the basal fragment are linked together by metal–metal bonds, as well as by bridging carbonyl groups. While the cobalt and one rhodium atom of the basal triangle complete their coordination through two terminal carbonyl groups, the second rhodium is additionally linked to one terminal carbonyl group and to a phosphine ligand, which is *trans*-positioned (Co(2)–Rh(1)–P 170.4(1)°).

The six metal–metal bond distances are from 2.663(2) to 2.557(2) Å. For the bond distances involving the apical Co(2) atom, it is noteworthy that the value of the Co(2)–Rh(1) bond is somewhat longer than the other apical–basal Co(2)–Rh(2) bond (2.617(2) vs. 2.567(2) Å). An analogous lengthening of the metal–metal bond *trans* to the phosphine ligand has been found in $[Co_4(CO)_{11}(PPh_3)]$, which is isostructural with **3** [5]. It is also worth commenting on the fact that the non-bridged Rh–Co bond distances are shorter than the bridged Rh–Co distances, since it is commonly believed that the reverse situation prevails, viz. M–M bonds spanned by bridging carbonyl groups are generally shorter than unbridged ones [33]. However, analysis of the metal–metal bond lengths for the homometallic clusters in Table 1 show that a significant shortening of the bridged M–M bonds with respect to the unbridged ones is observed only for cobalt; for rhodium and iridium, the bridged bonds are longer or of the same lengths as the unbridged bonds.

Experimental

$[Co_3Rh(CO)_{12}]$ and $[Co_2Rh_2(CO)_{12}]$ were prepared as described previously [24]. Triphenylphosphite (Aldrich) was vacuum-distilled before use and triphenylphos-

phine (B.D.H.) was used as received. Elemental analyses were carried out at the University of Kent by Mr. A.J. Fassam. $^{31}P\{^1H\}$ NMR spectra in $CHCl_3$ were measured as described previously [34], and $\delta(P)$ is referenced to H_3PO_4 (85% in D_2O). All operations were carried out under a dinitrogen atmosphere using standard Schlenk tube techniques.

Preparation of $[Co_3Rh(CO)_{11}(PPh_3)]$

A solution of PPh_3 (170 mg; 0.65 mmol) in hexane (40 cm^3) was added dropwise to a solution of $[Co_3Rh(CO)_{12}]$ (400 mg; 0.65 mmol) in hexane (100 cm^3). There was an immediate reaction, and recrystallization at $-30\,^\circ C$ gave the product as pure black crystals which were collected by filtration, washed with a little cold hexane, and dried under vacuum. Found: C, 40.80; H, 1.71. $C_{29}H_{15}Co_3O_{11}PRh$ calcd.: C, 40.97; H, 1.78%.

Preparatioin of $[Co_3Rh(CO)_{11}\{P(OPh)_3\}]$

To a solution of $[Co_3Rh(CO)_{12}]$ (340 mg; 0.55 mmol) in hexane (100 cm^3) was added dropwise a solution of $P(OPh)_3$ (171 mg; 0.55 mmol) in hexane (20 cm^3). The IR spectrum of the mixture showed the immediate formation of the product, which unfortunately could only be obtained as an oil, and this was used for the ^{31}P NMR measurements.

Preparation of $[Co_2Rh_2(CO)_{11}(PPh_3)]$

PPh_3 (160 mg; 0.61 mmol) in hexane (30 cm^3) was added dropwise to a solution of $[Co_2Rh_2(CO)_{12}]$ (400 mg; 0.61 mmol) in hexane (50 cm^3). After 30 min, a slight precipitate had formed, and storing this solution at $-30\,^\circ C$ gave large black crystals of the product which were used for X-ray analysis.

Preparation of $[Co_2Rh_2(CO)_{10}(PPh_3)_2]$

PPh_3 (320 mg; 1.22 mmol) in hexane (30 cm^3) was added dropwise to a solution of $[Co_2Rh_2(CO)_{12}]$ (400 mg; 0.61 mmol) in hexane (50 cm^3). This was stirred overnight and the resulting precipitate was collected by filtration and recrystallised from CH_2Cl_2 and hexane to give the desired product.

Preparation of $[Co_2Rh_2(CO)_{12-x}(P(OPh)_3)_x]$ ($x = 1$ or 2)

To a solution of $[Co_2Rh_2(CO)_{12}]$ (50 mg; 0.08 mmol) in $CDCl_3$ (2 cm^3) in an NMR tube at $-78\,^\circ C$ was added $P(OPh)_3$ (24 mg; 0.08 mmol) in CD_2Cl_2 (2 cm^3). The NMR tube was then capped, warmed to room temperature for a few minutes, and then immediately cooled to $-50\,^\circ C$ for NMR measurements. This gave the monosubstituted derivative, as evidenced by both NMR and IR measurements. Using a similar procedure gave the bis-substituted derivative.

Crystal data and data collection

$C_{29}H_{15}Co_2PRh_2$, $M = 894.1$, monoclinic, a 15.470(8), b 17.242(9), c 11.937(7) Å, β 100.65(8)°, U 3129.1 $Å^3$, space group $P2_1/n$, $Z = 4$, D_c 1.897 g cm^{-3}, $F(000) = 1744$, $\mu(Mo\text{-}K_\alpha)$ 21.7 cm^{-1}.

A well-formed crystal of dimension $0.32 \times 0.46 \times 0.50$ mm was selected for intensity data collection on a Philips PW 1100 diffractometer. The cell dimensions were determined by the least-squares refinement of the setting angles of 23 carefully

centred reflections. Data collection was carried out using the ω-2θ scan technique, within 2θ 50°. The scan speed was 0.08° s^{-1} and the scan width was calculated according to the formula $A + B \tan\theta$, where A 0.9° and $B = 0.3$. Stationary background measurements were taken before and after each scan for a time equal to half the scan time. The intensities of three reflections, measured every 2 h, showed no significant trend. The intensities were assigned standard deviations, calculated by using the value of 0.03 for the instability factor p [35]. The intensities were corrected for Lorentz polarization and absorption effects [36].

Solution and refinement of the structure. All the calculations were carried out on a SEL 32/77 computer by using the SHELX 76 [36] and ORTEP programs [37]. Neutral atom scattering factors were taken from ref. 38 for the non-hydrogen atoms and from ref. 39 for hydrogen atoms. Both the $\Delta f'$ and $\Delta f''$ component of anomalous dispersion were included for all non-hydrogen atoms [40]. The refinement was based on F_o, the function minimized being $\Sigma w(|F_o| - |F_c|)^2$ [36], where

Table 4

Positional parameters ($\times 10^4$ for atoms other than H, $\times 10^3$ for H) for (**3**)

Atom	x	y	z	Atom	x	y	z
Rh(1)	1324(1)	2546(1)	1539(1)	C(1,1)	−584(6)	3418(4)	2039(9)
Rh(2)	663(1)	1736(1)	−321(1)	C(2,1)	−1444(6)	3149(4)	1718(9)
Co(1)	1675(1)	1046(1)	1409(1)	C(3,1)	−2090(6)	3632(4)	1110(9)
Co(2)	2320(1)	2014(1)	164(2)	C(4,1)	−1874(6)	4383(4)	824(9)
P	326(2)	2817(2)	2727(3)	C(5,1)	−1014(6)	4651(4)	1146(9)
O(1)	2295(9)	4040(8)	1883(12)	C(6,1)	−368(6)	4169(4)	1753(9)
O(2)	819(9)	1820(8)	−2716(12)	C(1,2)	−158(6)	1957(5)	3270(7)
O(3)	−1277(9)	1497(7)	−798(11)	C(2,2)	−53(6)	1826(5)	4440(7)
O(4)	3369(9)	238(8)	1630(11)	C(3,2)	−411(6)	1164(5)	4846(7)
O(5)	879(9)	−41(8)	2843(12)	C(4,2)	−874(6)	632(5)	4080(7)
O(6)	3957(9)	2349(8)	1754(12)	C(5,2)	−979(6)	763(5)	2910(7)
O(7)	2221(9)	3420(8)	−1245(12)	C(6,2)	−620(6)	1425(5)	2504(7)
O(8)	2790(8)	799(7)	−1341(11)	C(1,3)	739(5)	3363(5)	4021(8)
O(9)	197(7)	3426(7)	−427(10)	C(2,3)	1627(5)	3328(5)	4527(8)
O(10)	2564(9)	1823(8)	3502(12)	C(3,3)	1920(5)	3687(5)	5575(8)
O(11)	897(7)	46(7)	−525(10)	C(4,3)	1327(5)	4081(5)	6119(8)
C(1)	1898(9)	3482(8)	1785(12)	C(5,3)	439(5)	4117(5)	5613(8)
C(2)	744(10)	1813(9)	−1805(14)	C(6,3)	146(5)	3758(5)	4564(8)
C(3)	−524(10)	1584(9)	−570(13)	H(21)	−159(1)	264(1)	191(1)
C(4)	2698(11)	532(9)	1555(14)	H(31)	−268(1)	345(1)	89(1)
C(5)	1182(10)	388(9)	2318(13)	H(41)	−231(1)	471(1)	41(1)
C(6)	3332(10)	2218(9)	1157(13)	H(51)	−87(1)	516(1)	95(1)
C(7)	2268(10)	2872(9)	−681(14)	H(61)	22(1)	435(1)	197(1)
C(8)	2642(10)	1266(9)	−762(13)	H(22)	26(1)	219(1)	496(1)
C(9)	531(9)	2891(8)	58(12)	H(32)	−34(1)	107(1)	564(1)
C(10)	2085(10)	1801(9)	2649(14)	H(42)	−112(1)	18(1)	436(1)
C(11)	1028(10)	615(9)	−32(13)	H(52)	−129(1)	40(1)	239(1)
				H(62)	−69(1)	151(1)	171(1)
				H(23)	203(1)	306(1)	416(1)
				H(33)	252(1)	366(1)	592(1)
				H(43)	153(1)	433(1)	683(1)
				H(53)	4(1)	439(1)	598(1)
				H(63)	−46(1)	378(1)	422(1)

$w = 1/\sigma^2(F_o)$. The structure was solved by the heavy atom method, a Patterson map showing the position of two rhodium atoms. Successive Fourier syntheses revealed all the non-hydrogen atoms. Full-matrix least-squares refinements were carried out assigned anisotropic thermal parameters to the rhodium, cobalt and phosphorus atoms. The phenyl rings of the triphenylphosphine ligand were treated as rigid groups and the hydrogen atoms, introduced in their calculated positions, were not refined. At convergence, the final R and R_w factor values were 0.077 and 0.078 for 4179 reflections having $I \geq 3\sigma(I)$. The atomic coordinates are given in Table 4.

Acknowledgement

We thank C.N.R. and S.E.R.C. for support; a quota award from S.E.R.C. (to S. Johnson) and for a CASE Studentship (to M. Bojczuk). We also thank Drs. Whyman and Fakely for useful discussions.

References

1 F.H. Carré, F.A. Cotton and B.A. Frenz, Inorg. Chem., 15 (1976) 380.
2 C.H. Wei, Inorg. Chem., 8 (1969) 2384.
3 M.J. Went, C.P. Brook and D.F. Shriver, Organometallics, 5 (1986) 755.
4 V.G. Albano, D. Braga, G. Longoni, S. Campanella, A. Ceriotti and P. Chini, J. Chem. Soc. Dalton Trans., (1980) 1820.
5 D.J. Darensbourg and M.J. Incorvia, Inorg. Chem., 20 (1981) 1911.
6 K. Bartl, R. Boese and G. Schmid, J. Organomet. Chem., 206 (1981) 331.
7 E. Keller and H. Vahrenkamp, Chem. Ber., 114 (1981) 1111.
8 B.T. Heaton, L. Longhetti, D.M.P. Mingos, C.E. Briant, P.C. Minshall, B.R.C. Theobald, L. Garlaschelli and U. Sartorelli, J. Organomet. Chem., 213 (1981) 333.
9 G. Ciani, L. Garlaschelli, M. Manassero and U. Sartorelli, J. Organomet. Chem., 129 (1977) C25.
10 G. Ciani, M. Manassero and A. Sironi, J. Organomet. Chem., 199 (1980) 271.
11 L. Garlaschelli, S. Martinengo, P. Chini, F. Canziani and R. Bau, J. Organomet. Chem., 213 (1981) 379.
12 F. DeMartin, M. Manassero, M. Sansoni, L. Garlaschelli, C. Raimondi, S. Martinengo and F. Canziani, J. Chem. Soc. Chem. Commun., (1981) 528.
13 G. Ciani, M. Manassero, V.G. Albano, F. Canziani, G. Giordano, S. Martinengo and P. Chini, J. Organomet. Chem., 150 (1978) C17.
14 V.G. Albano, P.L. Bellon and V. Scatturin, J. Chem. Soc. Chem. Commun., (1967) 730.
15 D.J. Darensbourg and B.J. Baldwin-Zuschke, Inorg. Chem., 20 (1981) 3846.
16 A.J. Blake and A.B. Osborne, J. Organomet. Chem., 260 (1984) 227.
17 E. Iiskola and T. Pakkanen, Acta Chem. Scand., A, 38 (1984) 731.
18 B.T. Huie, C.B. Knobler and H.D. Kaesz, J. Am. Chem. Soc., 100 (1978) 3059; R.G. Teller, R.D. Wilson, R.K. McMullan, T.F. Koetzle and R. Bau, ibid., 100 (1978) 3071.
19 J.P. Pursianen, T.A. Pakkanen and J. Jääskeläinen, J. Organomet. Chem., 290 (1985) 85.
20 A.S. May, Ph.D. thesis 1986, University of Western Australia.
21 B.T. Heaton, Am. Chem. Soc. Symp. Ser., 211 (1983) 227.
22 B.T. Heaton, L. Strona, R. Della Pergola, L. Garlaschelli, U. Sartorelli and I.H. Sadler, J. Chem. Soc. Dalton Trans., (1983) 173.
23 V.G. Albano, G. Ciani and S. Martinengo, J. Organomet. Chem., 78 (1974) 265.
24 S. Martinengo, P. Chini, F. Cariati and T. Salvatori, J. Organomet. Chem., 59 (1973) 379.
25 J. Evans, B.F.G. Johnson, J. Lewis, T.W. Matheson and J.R. Norton, J. Chem. Soc. Dalton Trans., (1978) 626.
26 J. Pursianen, T.A. Pakkanen, B.T. Heaton, C. Seregni and R.J. Goodfellow, J. Chem. Soc. Dalton Trans., (1986) 681.
27 J.D. Atwood, Inorganic and Organometallic Reaction Mechanisms, Brooks/Cole Publishing Company, Monterey, CA, 1985, p. 108.

28 T. Venäläi and T. Pakkanen, J. Organomet. Chem., 266 (1984) 269.
29 M. Bojczuk, Ph.D. thesis, University of Kent, 1986.
30 I.T. Horvath, Organometallics, 5 (1986) 2333.
31 H.E. Hosseini and J.F. Nixon, J. Organomet. Chem., 150 (1978) 129.
32 G.F. Stuntz, J.R. Shapley and C.G. Pierpont, Inorg. Chem., 16 (1978) 2596.
33 R. Colton and M.J. McCormick, Coord. Chem. Rev., 31 (1980) 1.
34 B.T. Heaton, L. Longhetti, L. Garlaschelli and U. Sartorelli, J. Organomet. Chem., 192 (1980) 431.
35 P.W.R. Corfield, R.J. Doedens and J.A. Ibers, Inorg. Chem., 6 (1976) 197.
36 G.M. Sheldrick, System of Computing Programs, University of Cambridge, Cambridge, England, 1976.
37 C.K. Johnson, Oak Ridge Natl. Lab. (Rep) ORLN (U.S.) ORNL-5138, 1976.
38 International Tables for X-ray Crystallography, Kynoch Press, Birmingham, England, IV, 1974, p. 99.
39 R.F. Stewart, E.R. Davidson and W.T. Simpson, J. Chem. Phys., 42 (1965) 3175.
40 International Tables for X-ray Crystallography, Kynoch Press, Birmingham, England, IV, 1974, p. 149.